

Applying a new synchronous inversion of seismograms using maximum likelihood method and stochastic refinements to study ultra-thin oil-saturated reservoirs

Aleksandr Konyushenko¹, Valery Shumilyak¹, Aleksander Inozemtsev^{2*} and Baurzhan Suleimenov² present a pre-stack inversion of seismograms to study ultrafine oil-saturated carbonate reservoirs at depths of 4 to 5 km in Belarus.

Seismic inversion makes use of single or multi-dimensional seismic trace data to derive elastic properties from seismic amplitude data. These elastic properties are subsequently used to make inferences about seismic lithology, lithologic properties, and the presence of fluids. Most implementations of seismic inversions operate on limited stacked subsets of the seismic data. Common inputs to inversion methods include angle stacks, offset stacks, or multiple stacks of time-lapsed data. The implementation in this paper makes use of a synchronous pre-stack inversion based on the maximum likelihood algorithm (Anat Canning and Alex Malkin, 2009). The PMLI inversion is applicable to time and depth angle or offset seismograms. It is a full pre-stack inversion, which inverts each and every trace of an offset or angle gather and returns elastic properties.

The PMLI inversion can also invert partial angular or offset sums, which can be created in any processing system. As a complete pre-stack inversion, PMLI provides higher accuracy and noise immunity as observed in the output results of P_w and S_w impedances, density, V_p/V_s , Poisson's ratio, Lambda Rho (LR) and Mu Rho (MR). PMLI also incorporates a necessary and effective preprocessing step, which is performed on-the-fly as part of the inversion process.

Because the PMLI method operates on gathers, it is easily and efficiently parallelized for multi-core and multi-node clusters and for shared memory architectures.

Brief technical description

PMLI is a complete synchronous pre-stack inversion. The formation of physical properties, I_p , I_s , Density, V_p and V_s , V_p/V_s , Poisson ratio, LR and MR, are extracted using inversion directly from the input seismograms. An optimum solution is found by minimizing the following functional:

$$J = J_b * W_b + J_s * (1 - W_b).$$

Here, J_b is the difference between the background model of impedances and the output impedances (a petrophysical term), J_s is the difference between the synthetic seismogram and the input seismogram (a seismic term), W_b is the background model-to-seismic weight ratio.

The algorithm is implemented as a perturbation and optimization process, where the optimization criterion is a weighted sum of the seismic (Zoeppritz) and geologic deviation terms. Therefore both the seismic and geologic terms undergo parallel minimization in the process of inversion, ensuring stability and likelihood of the result. The minimum of the objective function is found by the conjugate gradient method. Input data for the geologic background model originates from borehole surveys and includes I_p , I_s , Density, V_p , and V_s logs. The inversion can be carried out with or without a structural model.

A special seismogram preprocessing step is very important for the quality of the inversion results, as it provides additional benefits for seismograms of varying quality, such as signal-to-random/coherent noise ratio, vertical resolution, and moveout correction. The coherent noise includes surface and multiple energy. The preprocessing step also eliminates signal stretching along offsets or (incidence/reflection) entry angles.

Wavelets for the PMLI inversion can be loaded from external databases or from an ASCII file. The wavelet is evaluated and extracted based on calibration of real and synthetic seismograms, or on one-dimensional modelling using the angle sum of the mean entry angles (the entry angle range is set up by the user). An amplitude calibration factor, which reduces the seismic data amplitude level to the synthetic data, is automatically determined at this stage. An additional stretch elimination feature is used automatically in the process of inversion. To use the feature, the geophysicist indicates a specific reference entry angle (e.g.,

¹ RUP PO Belorusneft.

² Paradigm Moscow.

* Corresponding Author, E-mail: alexander.inozemtsev@PDGM.com

Experience the Energy

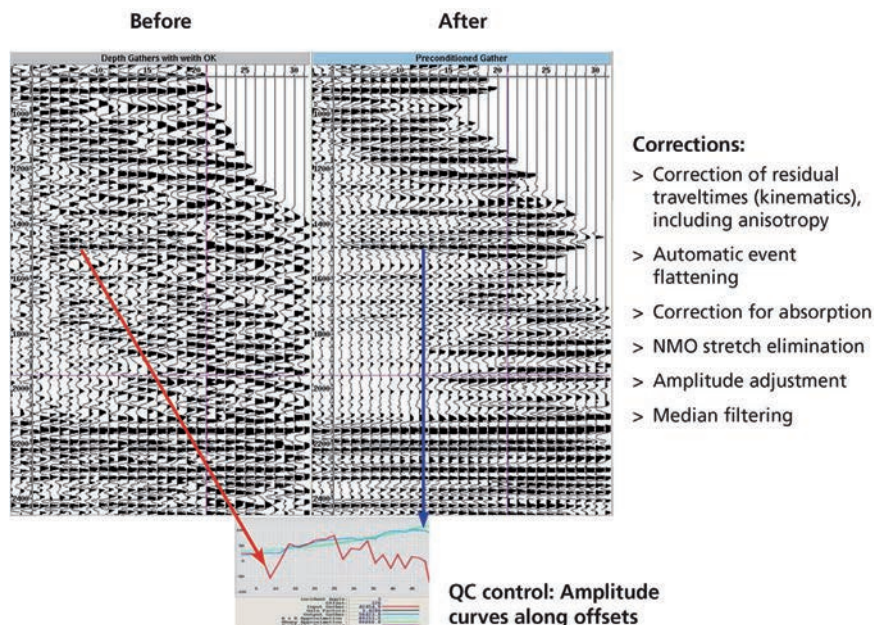


Figure 1 Example of the result of special preprocessing used to improve the quality of the input seismograms and control the quality of the result with a low signal-to-noise ratio (SNR = 1-1.3).

15 degrees), which will be used as a reference for eliminating the signal stretching for all other angles.

The geophysicist can obtain I_p , I_s , Density, V_p and V_s , V_p/V_s , Poisson's ratio, LR and MR for the inversion output. For quality control purposes, the geophysicist can request synthetic seismograms and residual seismograms, which are also automatically generated in the inversion process. The geophysicist sets up the structure of the seismograms (multiplicity, entry angle range, entry angle increment) before running the inversion.

Figures 2 and 3 illustrate examples of synthetic seismograms generated for PMLI inversion quality control with a signal-to-noise ratio that is high and low, respectively. The data were obtained in Western Siberia. The second example shows a residual seismogram, which has discrepancies between the seismic data and synthetic data, and in this case, contains mainly regular and random noise amplitudes.

Application to ultra-thin reservoirs

Results of PMLI field testing and stochastic refinement of the results are provided below, from a project involving investigation of ultra-thin carbonate reservoirs in the geological conditions of Belarus.

The object of the study was a subsalt oil deposit confined to a structural and tectonic trap consisting of two blocks (I and II), separated by a dislocation of about 60 m (Figure 4).

The seismic acquisition was designed to detail the geological structure of intersalt and subsalt sediments, to map the structure-forming fractures, and to discover and delineate traps that can potentially contain oil and gas in the intersalt and subsalt Devonian formations. Coverage for the 3D

seismic survey is 120 km² with a fold of 100 and bin spacing of 20 m. The maximum offset is 4000 m.

The cross-section of the lithologies within the deposit consists of an Archean Proterozoic crystalline basement and Upper Proterozoic, Paleozoic, Mesozoic and Cenozoic sedimentary formations. The sedimentary cover structure is characterized by the presence of two salt-bearing strata, Lebedyanko-Polesky and Evlanovsko-Livensky, with terrigenous and carbonate subsalt formations, as well as lower saliferous, intersalt, upper saliferous, and suprasalt formations, which can be identified for those strata.

The commercial oil content of the deposits is associated with the subsalt carbonate deposits (Voronezh, Semiluksky, Sargaevsky). The main oil deposit here is confined to the Semiluksky horizon sediments.

The oil deposit over the surface of the productive subsalt sediments is in the form of an uplift, defined on the northern, western, southern and south-eastern sides, by disjunctive dislocations with the amplitudes of 180, 170, 120, and 200 m, respectively. The structure is divided into two blocks (western and eastern) by a sub-meridional fault with a throw of about 70 m (Figure 3a).

Semiluksky productive deposits are composed of rocks from brownish-grey, brownish-dark grey, irregularly argillaceous dolomite to pelitomorphic fine-grained, brecciated and dense marl with poorly defined lamination. Rare caverns and fissures are healed with anhydrite and crystalline dolomite.

The reservoirs are porous and cavernous secondary dolomites, which are fractured in some areas and confined to the upper and middle part of the horizon. The reservoirs are of a mixed type: cavernous/porous, porous/cavernous, and cavernous/porous/fractured.

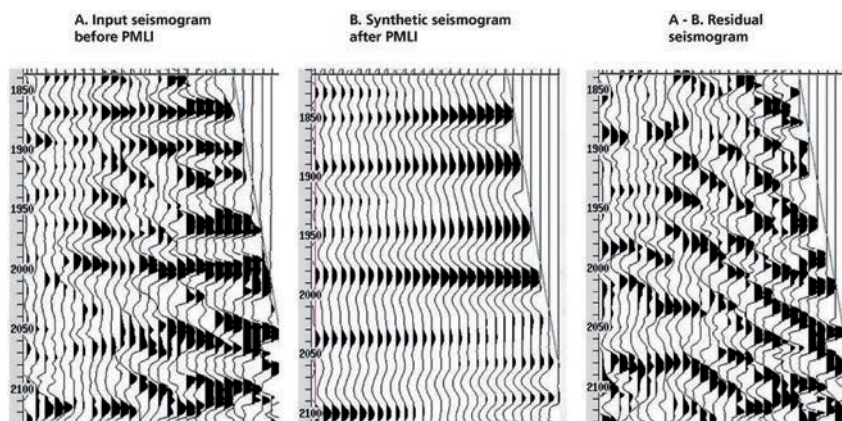
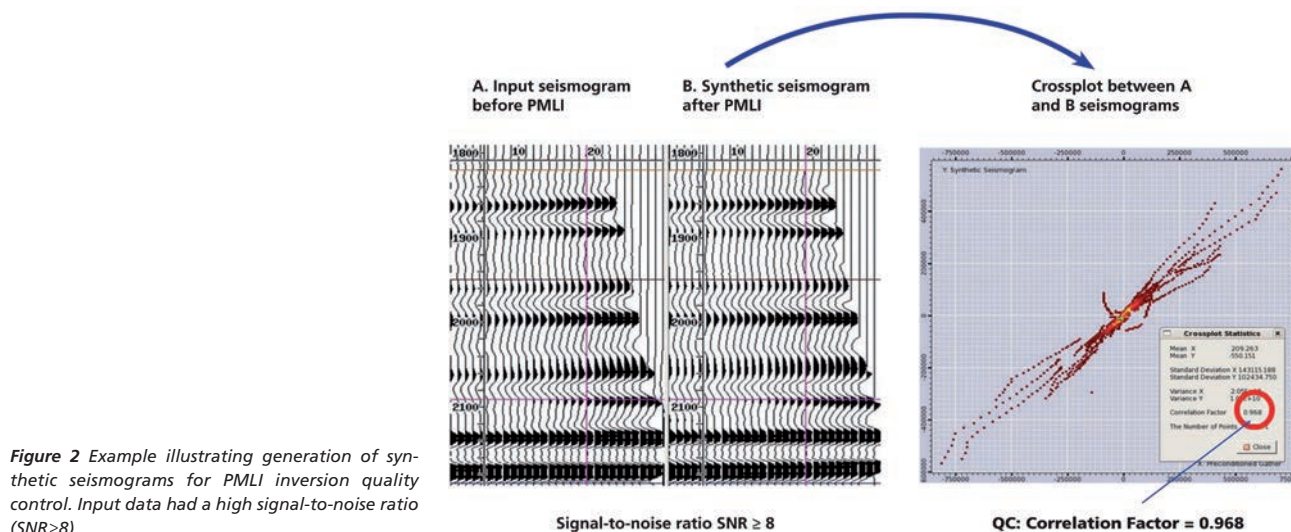


Figure 3 Example illustrating generation of synthetic seismograms for PMLI inversion quality control. Input data had a low signal-to-noise ratio ($SNR \leq 1$).

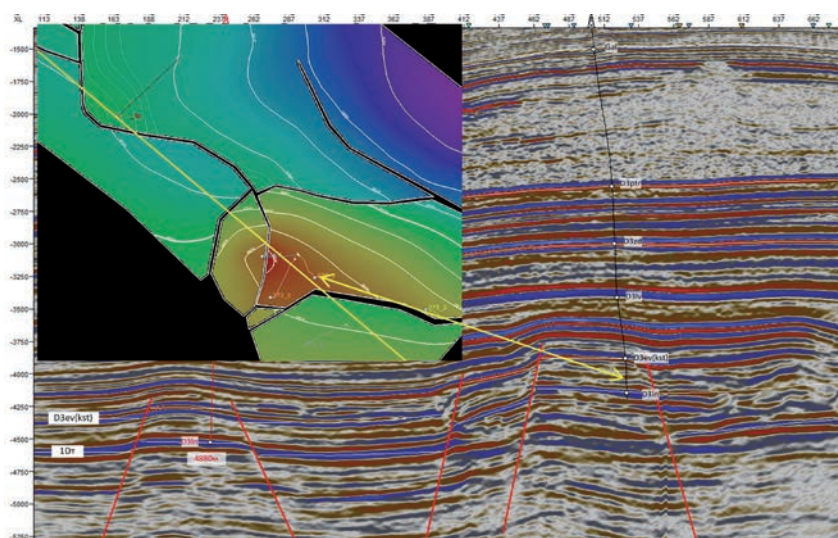


Figure 4 Fragment of a structural map of the sub-salt terrigenous formation surface and vertical 3D cube section across the deposit.

The reservoir within the deposit is widespread, but the non-uniform effects of the leaching processes and fracturing have resulted in a chaotic and patchy distribution of high-capacity

carbonates over the Semiluksky deposit area. The total thickness of the reservoir beds varies from 8.4 m to 15.6 m, and the weighted mean accessible porosity ranges from 4.5% to 9.7%.

Experience the Energy

The main objective of the project was to detect and detail the zones of enhanced reservoir properties in the ultra-thin hydrocarbon-saturated beds that are up to 5-m thick. The seismogram quality is described by an initial average signal-to-noise ratio of 1.5 with an effective spectrum width of 10-80 Hz. The maximum entry angle at a depth of 4300 m for the main target horizon is about 32 degrees.

To improve the quality of the input seismograms, a special preprocessing phase was used in the inversion process, and the results are shown in Figure 5.

The preprocessing improved the signal-to-noise ratio to 5.3 by suppressing, to a large extent, the coherent noise, including multiple waves. The preprocessing also stabilized the signal waveform and amplitude behaviour along offsets. Evaluation of the signal waveform for inversion shows that it is close to the zero-phase.

The geologic (petrophysical) model results from the PMLI inversion for this project are discussed below. Longitudinal sections of volumes of the basic petrophysical properties obtained from the PMLI inversion output near a productive (oil) well are shown below (Figure 6). Comparison of different properties shows that the zone with lower I_p impedance values corresponds to the oil saturated strata, whereas the S-wave impedance values, I_s , did not

practically change in the same zone. The density values also do not differ substantially from the trend values, which can be explained by an absence of large (distant) entry angles (of 32-50°) in the trace data. There is an ample amount of factual data in the literature, which shows that the information on a sharp change (lowering) of density indicative of reservoir saturation with hydrocarbons is indeed reflected by the amplitudes of the traces within the range of distant entry angles. These changes are much sharper than changes in the velocity within the same range of the entry angles. In another project carried out in the same area, the density values extracted from seismograms by inversion, which were in the range of 30-45°, correlated with 60 to 70% oil saturation in wells.

Unlike impedance and velocity values, the Lamé parameters (LR and MR), showed a sharp anomaly between them, which suggests that these parameters indicate hydrocarbon saturation. The velocity ratio, V_p/V_s , and Poisson's ratio also show sharp low-value anomalies in the reservoir hydrocarbon saturation zone.

It is worth noting that AVO attributes (Gradient, Poisson reflectivity, Lambda Rho, and Mu Rho) also proved informative in the project, which is a rare case for a carbonate reservoir. A cross-plot between the NIR attributes and

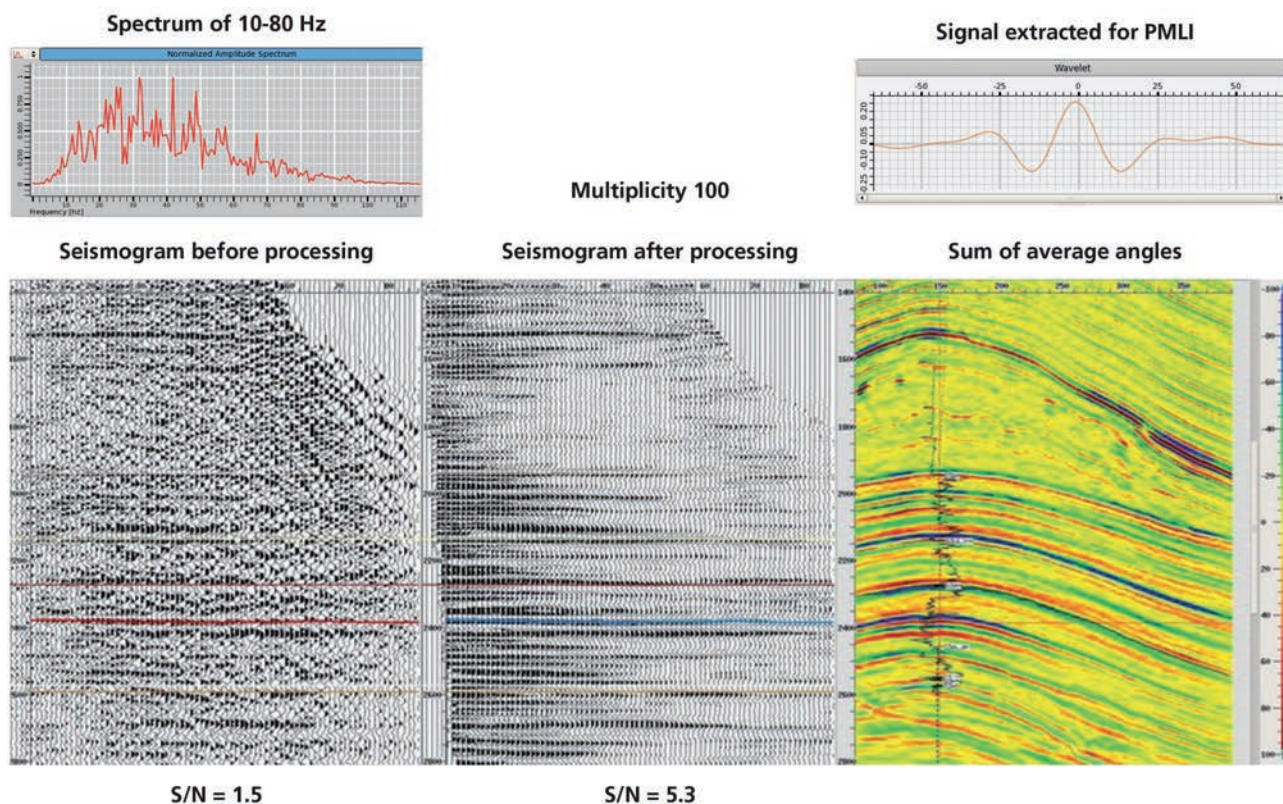


Figure 5 Improving the quality of the initial seismograms using preprocessing at the first stage of the PMLI inversion. Evaluation of the signal waveform based on calibration of the synthetic and seismic data (the cross-section of the mean entry angles) is shown in the right hand part of the illustration. Carbonate reservoirs Belarus.

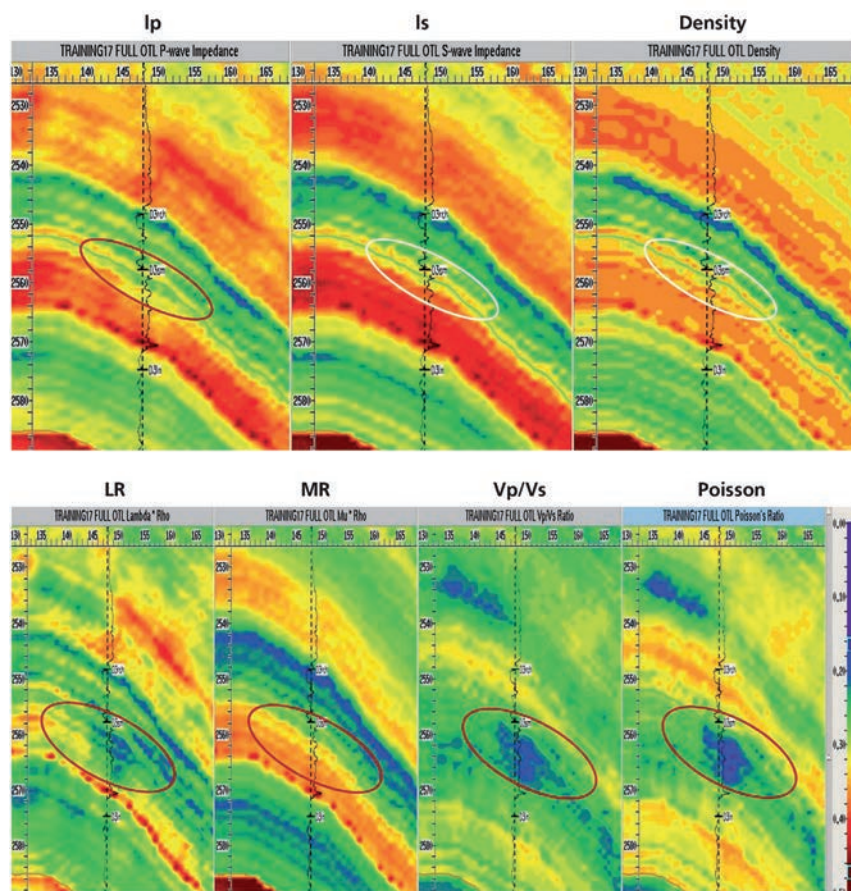


Figure 6 Longitudinal section of cubes of the physical properties I_p , I_s , Density, V_p and V_s , V_p/V_s , Poisson ratio, LR and MR, obtained at the PMLI inversion output near a productive (oil) well. A target interval (dolomitized porous/cavernous/fractured limestone) of the reservoir containing thin oil-saturated strata is highlighted with an oval.

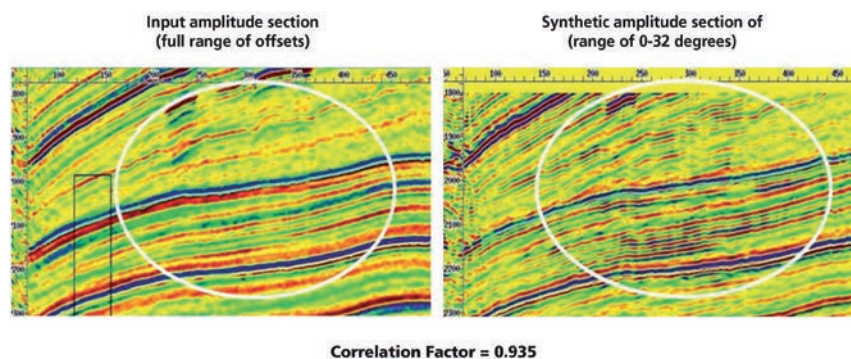


Figure 7 Correlation coefficient assessment for PMLI inversion global control. Comparison of sections of the amplitudes obtained from the initial seismograms and from the output synthetic seismograms that were obtained after PMLI inversion.

the gradient clearly shows the anomalous zones that are classified as Class IV AVO hydrocarbon saturated reservoirs. This is due to the fact that the carbonate reservoirs and overlying strata have rarely occurring structures with almost the same lithological features. The actual caprock for porous/cavernous-fractured reservoirs is a fairly thick layer of dense impermeable dolomite overlain on top with clay seams. The reflectance values calculated using the acoustics data and density logs are within the range of 1.1 to 1.3, and significant changes in the V_p/V_s ratio were also observed. With these values of the above-mentioned parameters, the Shui or Aki-Richard binomial approxima-

tions for offsets of up to 30° show good convergence with the Zoeppritz equation.

The PMLI inversion was controlled locally (in the wells) and globally by comparing the section obtained based on the synthetic seismograms with the original section, obtained from the initial seismograms (Figure 7). There is a noteworthy feature of the global control that is significant. A section plotted based on the synthetic seismogram output has a higher vertical and lateral resolution. More specifically, this section shows a structural discontinuity of tapering out zones better than the initial seismogram section. This synthetic section is useful for refining the correlation and

Experience the Energy

for finer detailing of complex areas in the seismic section. This effect is due to the combined influence of the powerful preprocessing and inversion on the result.

Evaluation of the vertical resolution at the PMLI inversion output based on volumes of I_p impedance values (Figure 8) in the main reservoir interval showed that the minimum thickness of the reservoir that is being identified ranges from 5 to 9 m. For evaluation, the sample values were extracted from the volumes of impedance data analyzed in the deep area, and compared with the acoustic impedance curves obtained in the wells (Figure 9).

Accordingly, the resolution of the seismic impedance was $dH = 5-9$ m. These estimates are consistent with the following formula used for evaluating the vertical resolution in the time domain (Kondratyev, 1995), which was upgraded by the authors for a deep area:

$dH = 0.125 * V_{int} / (F_B - F_H)$, where dH is the bed thickness in metres; V_{int} is the reservoir interval velocity; $F_B - F_H$ is the width of the seismic signal spectrum.

These estimates show that the inversion result is also limited to the frequency range of the seismic signal. Further increase

of the vertical resolution is only possible with the use of stochastic (geostatistical) methods.

Figure 10 shows a map of seismic impedance and AVO attribute of Poisson's ratio. There is a correlation of low impedance, I_p , and zones with anomalies of the Poisson's ratio attribute both in the zone of oil producing Wells 1, 2, 3 and in the zone of water-saturated reservoirs (the reservoir in Well 4 is saturated with water). The lower impedance zone with the producing wells belongs to a structural uplift.

Stochastic refinement of properties (as applied to the I_p impedance)

The PMLI inversion gave a seismic impedance resolution (dH) of 5-9 m. The second part of the project was aimed at improving the vertical resolution of the seismic impedance to 1-2 m using the borehole data and stochastic methods. The stochastic or geostatistical inversion is currently the main tool for improving vertical resolution for a 3D study of reservoir property distribution. The following input data were used for the stochastic refinement: one volume of seismic impedance; four wells with logging data; borehole measurement data: D3ln, D3rch, D3sm; and seismic horizon D3ln as a trend.

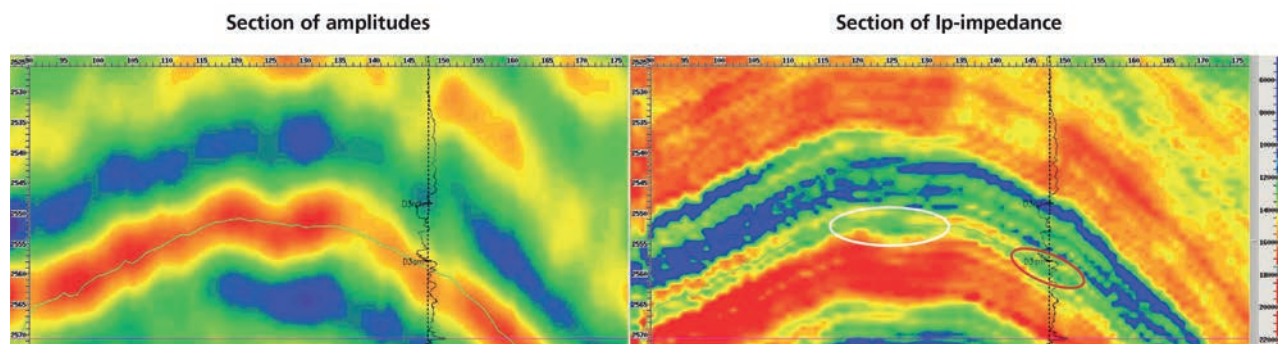


Figure 8 Longitudinal section from the amplitude volumes and I_p impedance values from the PMLI inversion output. A red oval highlights the zones of major oil-saturated reservoirs. A white oval highlights a zone of lower impedance values in the structure roof, which is promising for drilling.

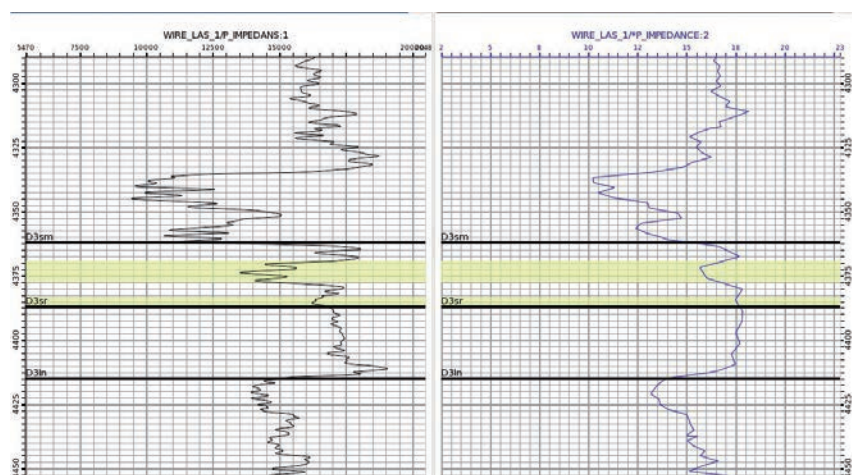


Figure 9 Comparison of acoustic impedance curves obtained in the well (A) with those extracted from the volumes of impedance value (B). The reservoirs are highlighted with yellow.

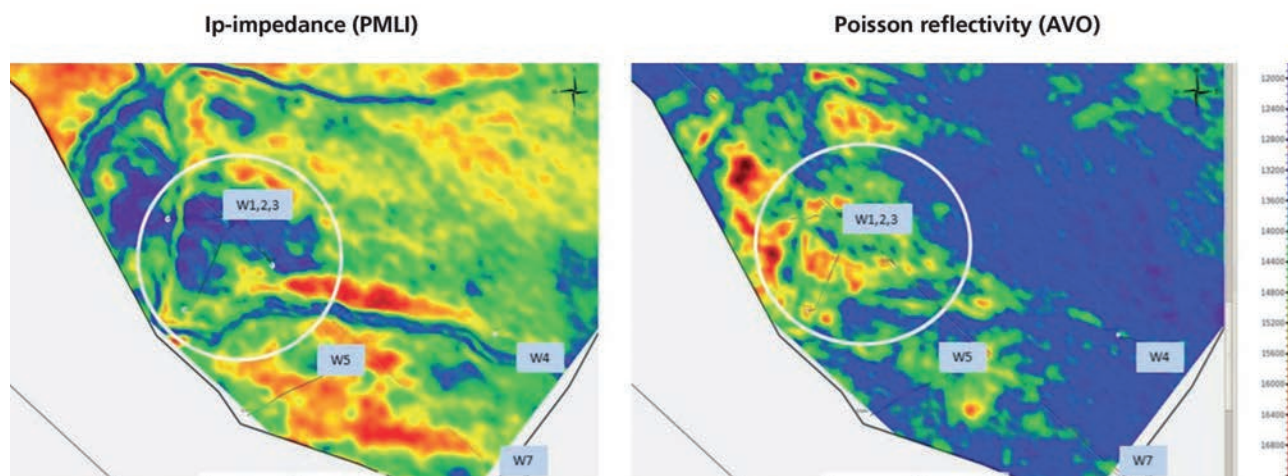


Figure 10 PMLI. Final map of the Ip impedance and Poisson's ratio extracted on the roof of the main reservoir D3sm. Wells 1, 2 and 3 are oil-saturated wells; Well 4 is a water-saturated well. A circle highlights an area of major zones of prospecting.

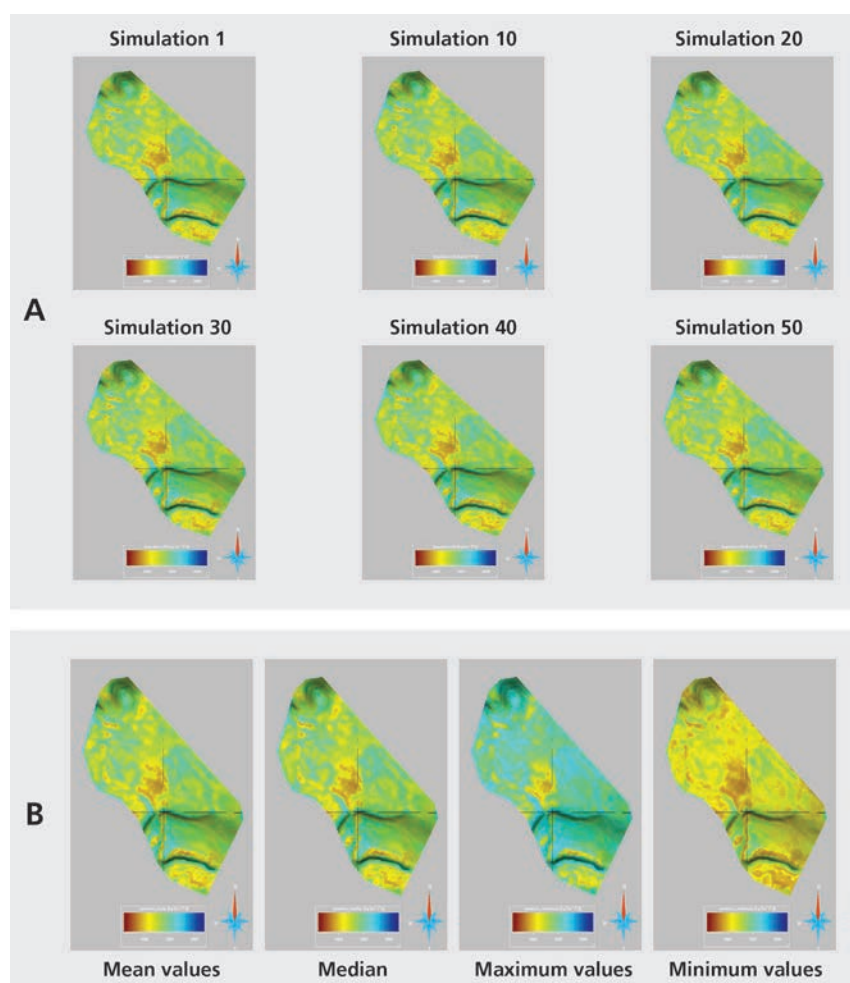


Figure 11 Analysis of the stochastic modelling results. a) Examples of individual simulations (every tenth simulation); b) Summary variants that were adopted for the final analysis and prediction.

A structural model was also used in the stochastic inversion and included a surface for the D3ln trend, and

a geological grid that consisted of two beds – D3rch and D3sm with a thickness ($dH = 80$ ms, $dT = 30$ ms).

Experience the Energy

The geological grid is displayed with a lateral cell size of 40x40 m. The vertical size is 0.2 m/s and the total number of cells is about 11 million.

Seismic impedance in the form of a stratigraphic grid was imported into a simulation package. A combined analysis of the data was then conducted, and correlations between the seismic impedance values within the D3rch and D3sm intervals in the four wells were evaluated, showing an overall correlation coefficient of 0.9.

A detailed reservoir data analysis was then conducted. Histograms showing impedance distribution within the target intervals were obtained and the stochastic distribution was studied. The histograms were smoothed and azimuthal variograms (taking into account the structural trend) were obtained for 3D interpolation of data. The correlation radius range was determined to be 3.6-3.8 km.

Fifty simulations (implementations) were carried out with a variety of methods including a filling method, Sequential Gaussian Simulation, Kriging, and Collocated Cokriging. The correlation coefficient was 0.6. with the seismic impedance used as a trend. Summary variants of all

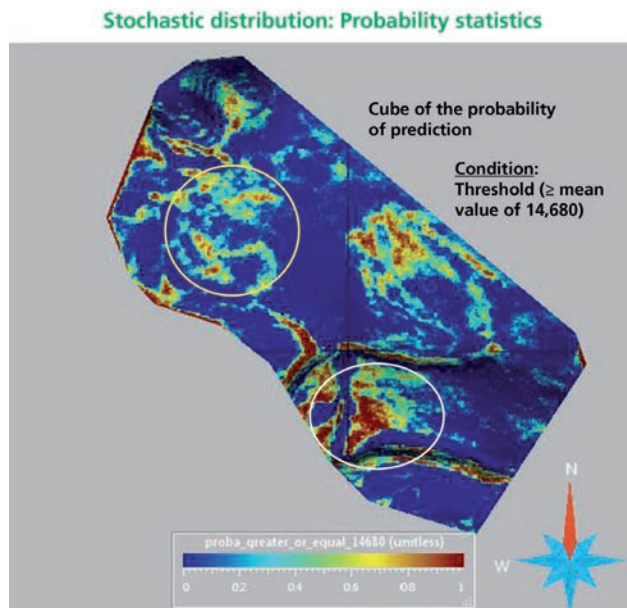


Figure 12 Cube of the probability of prediction for a preset threshold of \geq average value of I_p impedance of 14,680.

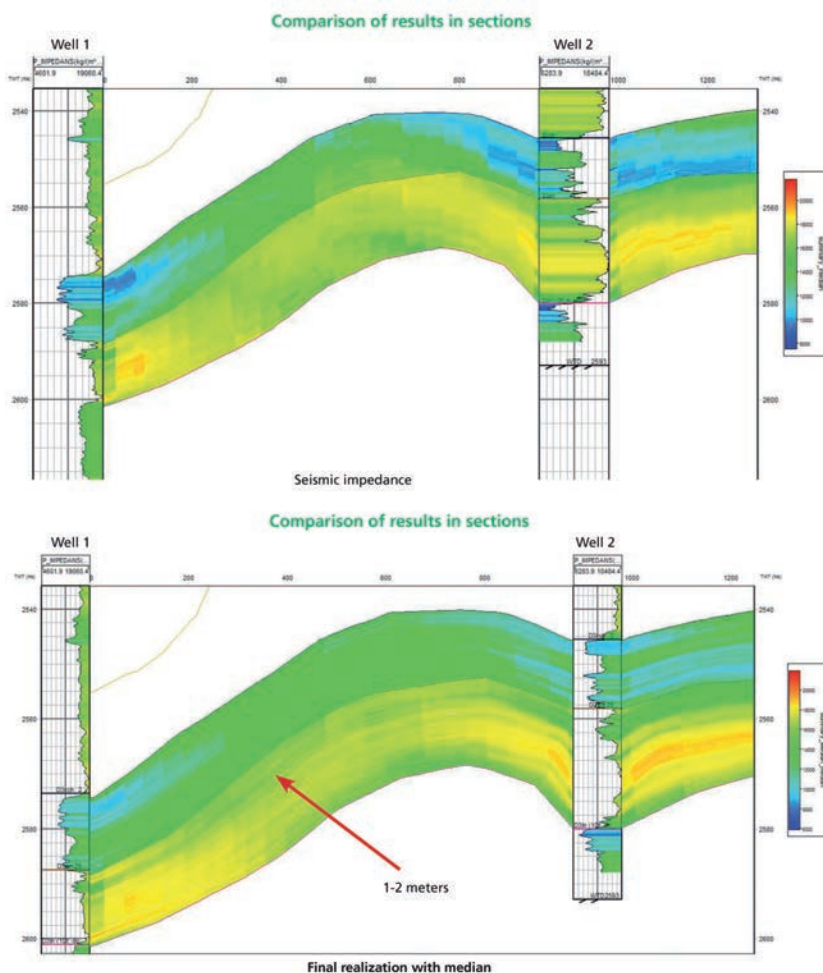


Figure 13 Example of a comparison between a seismic impedance, a) and stochastic impedance (in the median version), b) for the longitudinal section cut through two production wells.

simulations were also obtained for each cell based on the average, median (optimum prediction), minimum (best-case prediction) and maximum (worst-case prediction) values.

Figure 11 shows examples of individual simulations (each tenth simulation) and summary variants that were adopted for the final analysis and prediction. It should be noted that individual simulations show a good degree of similarity between them, which is a sign of stability of the stochastic modelling and good quality of the input data. At the same time, they differ in details.

The stochastic modelling was controlled using histograms of deviations and a cube of standard deviations. A cube of the probability of prediction was plotted as the stochastic modelling output (the most important stochastic modelling parameter) for a given threshold (\geq average value of impedance of 14,680 (Figure 12)). A cube of the probability of prediction allowed us to identify the most

promising zones for drilling at the final level of interpretation.

An example comparing a longitudinal section through the production wells between the seismic impedance, A, and the stochastic impedance (in the median version), B, is given below (Figure 13). The example shows that the stochastic version not only improves the vertical resolution between the wells to 1-2 m, but also enhances the lateral resolution or better traceability of thin beds between the wells. This is a valuable result of stochastic refinement.

Evaluation of the vertical resolution of the stochastic impedance, made in a stratigraphic grid in the area of the highest probability of prediction, shows that we do have a maximum resolution of up to 1-2 m in the beds (Figure 14). In fact, the improved resolution makes new and important details of the deposits visible. For example, there is an obvious separation of the section, based on the impedance

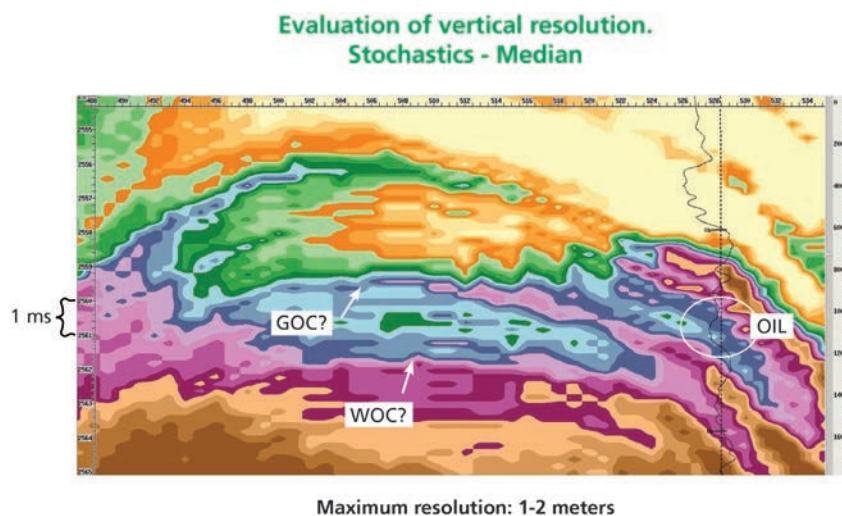


Figure 14 Evaluation of the vertical resolution of the stochastic impedance made in a stratigraphic grid in the area of highest prediction probability.

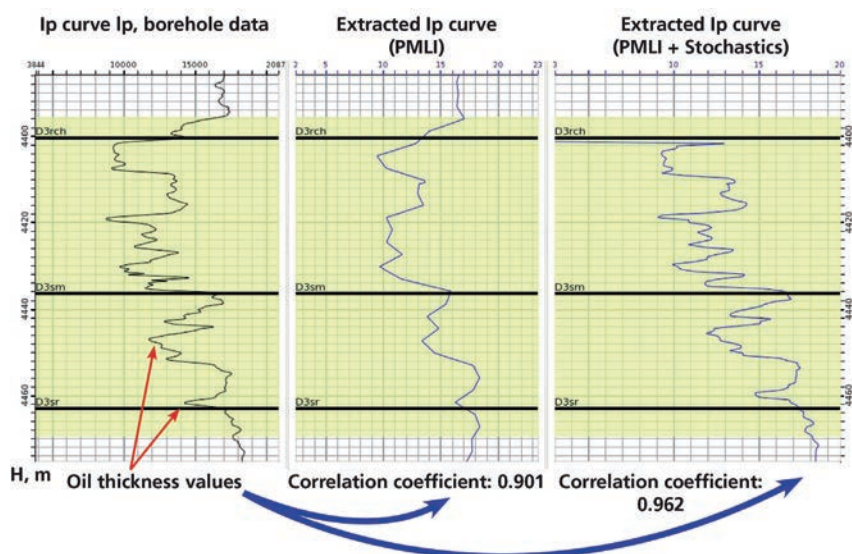


Figure 15 The local impedance quality control after the PMLI inversion and stochastic refinement near an oil-saturated well. The depth of the main oil-saturated interval is 4300 m.

Experience the Energy

values, into three zones: upper, middle and lower. These can be associated with different filling fluids: water in the bottom zone; oil in the middle zone; and gas condensate in the upper zone.

The local impedance quality control after the PMLI inversion and stochastic refinement near an oil-saturated well (Figure 15) also shows a higher vertical resolution of the stochastic version of the impedance.

Conclusions

The main geological result of this pilot/field trial shows the capabilities of the new inversion technology in improving the reliability of oil saturation prediction in thin reservoirs and at great depths. Thin reservoirs occurring at great depths represent a common situation with oil and gas deposits in the area of Belarus. The total thickness values for the subsalt reservoirs of the vast majority of the deposits rarely exceed 15-20 m. The results of this pilot/field trial were considered when a planned well placement was done in a tectonically screened structure discovered by conducting 3D operations in the northwestern part of an area under study (Figures 4, 12). They will be used for future drilling of production wells in the field (Figures 4, 12).

Regarding the inversion technology, the PMLI inversion was able to ensure a resolution of the seismic impedance (5-9 m) which could be stochastically refined to less than 5m resolution with a high correlation coefficient (1-2 m). The PMLI inversion is a quick procedure, and can be completed for the aforesaid project in eight hours. The inversion running time on 80 cores is a little more than one hour. It takes about four hours on 80 cores to run the PMLI inversion for a project covering 500 km², with the same fold.

The stochastic result refinement in this project took about 12 hours, including the preprocessing phase, simulation calculation, and result analysis.

Acknowledgements

The authors express their gratitude to Maksim Telelyuhin and Aleksey Gritsenko of Paradigm for their technical and software support they provided during the project implementation.

References

- Canning, A. and Malkin, A. [2011] *Pre-stack Maximum Likelihood Inversion*. EAGE.
- Yakovlev, I.V., Ampilov, P. and Filippova, K.E. [2011] Almost everything about seismic inversion, Part 2. *Seismic Technology*, 8 (1), 5-15.



blueback reservoir
GeoScience Solutions Partner

How do you monitor your Petrel* ecosystem?
Blueback Reservoir data management solutions enables better control and optimization of the Petrel software platform

EAGE
stand #2150

*Mark of Schlumberger

Blueback Reservoir
E sales@blueback-reservoir.com | T +47 51 37 35 00
blueback-reservoir.com